

Controlled fabrication of micropatterned supramolecular gels by directed self-assembly of small molecular gelators

Wang, Yiming; Oldenhof, Sander; Versluis, Frank; Shah, Maulik; Zhang, Kai; van Steijn, Volkert; Guo, Xuhong; Eelkema, Rienk; van Esch, Jan H.

DOI

[10.1002/smll.201804154](https://doi.org/10.1002/smll.201804154)

Publication date

2019

Document Version

Final published version

Published in

Small

Citation (APA)

Wang, Y., Oldenhof, S., Versluis, F., Shah, M., Zhang, K., van Steijn, V., Guo, X., Eelkema, R., & van Esch, J. H. (2019). Controlled fabrication of micropatterned supramolecular gels by directed self-assembly of small molecular gelators. *Small*, 15(8), Article 1804154. <https://doi.org/10.1002/smll.201804154>

Important note

To cite this publication, please use the final published version (if applicable).
Please check the document version above.

Copyright

Other than for strictly personal use, it is not permitted to download, forward or distribute the text or part of it, without the consent of the author(s) and/or copyright holder(s), unless the work is under an open content license such as Creative Commons.

Takedown policy

Please contact us and provide details if you believe this document breaches copyrights.
We will remove access to the work immediately and investigate your claim.

Controlled Fabrication of Micropatterned Supramolecular Gels by Directed Self-Assembly of Small Molecular Gelators

Yiming Wang, Sander Oldenhof, Frank Versluis, Maulik Shah, Kai Zhang, Volkert van Steijn, Xuhong Guo,* Rienk Eelkema,* and Jan H. van Esch*

Herein, the micropatterning of supramolecular gels with oriented growth direction and controllable spatial dimensions by directing the self-assembly of small molecular gelators is reported. This process is associated with an acid-catalyzed formation of gelators from two soluble precursor molecules. To control the localized formation and self-assembly of gelators, micropatterned poly(acrylic acid) (PAA) brushes are employed to create a local and controllable acidic environment. The results show that the gel formation can be well confined in the catalytic surface plane with dimensions ranging from micro- to centimeter. Furthermore, the gels show a preferential growth along the normal direction of the catalytic surface, and the thickness of the resultant gel patterns can be easily controlled by tuning the grafting density of PAA brushes. This work shows an effective “bottom-up” strategy toward control over the spatial organization of materials and is expected to find promising applications in, e.g., microelectronics, tissue engineering, and biomedicine.

Directed molecular self-assembly (DMSA) has emerged as a promising approach to achieve spatial organization of materials from molecular to macroscopic length scale, showing enticing applications in, e.g., molecular robots,^[1] microelectronics,^[2] and energy materials.^[3] In recent years, some strategies toward DMSA have been developed. For instance, the employment of self-assembly systems that are sensitive to external stimuli such as light,^[4] enzymatic action,^[5] pH,^[6] and nucleation seeds,^[7] has led to DMSA by controlling the spatial distribution of these stimuli. Another example of DMSA is achieved by reaction-diffusion,^[8] i.e., molecular reactants are separately distributed in space and allowed to react after meeting by diffusion, leading to local self-assembly at a certain preprogrammed location. Despite the recent progress, a major challenge for

further advance lies in control of the spatial parameters of the self-assembled structures.^[9]

We have recently proposed a catalysis-responsive supramolecular self-assembly system that involves an in situ formation of hydrazone-based gelator (HA₃) from water-soluble tris-hydrazide (H) and aldehyde (A) (Figure 1). The rate of HA₃ formation can be remarkably increased by acid catalysis, thereby providing a handle to control subsequent gelation.^[10] Using this gelator system, we previously achieved surface confined formation of gels using surfaces modified with a monolayer of sulfonic acid that act as a catalyst for gelator formation.^[11] That system has, however, several limitations which hamper further progress. First, the spatial resolution of gel formation along the surface plane

is limited, presumably by the low interfacial catalytic activity. And second, the continuous growth of the gels along the surface normal to form 3D objects is hampered by adhesion of gel fibers to the surface, which blocks the influx of reagents to the catalytic surface. With these problems in mind, in this work, we aim to develop interfacial catalytic patterns that enable control over the growth of gels in all three dimensions, and additionally, to obtain a better understanding of the local reaction-diffusion coupled self-assembly process that is required for the rational design of DMSA systems.

To reach this goal, we hypothesized that the catalytic activity of the patterned catalyst needs to be increased and become tunable, while simultaneously the adhesion of the gel fibers onto the catalytic surface needs to be prevented to allow for continuous growth of the gel patterns. As a possible solution, we focused on surfaces patterned with catalytic polymer brushes. Polymer brushes composed of a surface densely grafted with polymer chains show considerable potential to effectively increase the catalytic activity by using acidic polymers,^[12] which would be beneficial for reinforcing the spatial controllability. Importantly, compared to self-assembled monolayers, the fabrication of polymer brushes can be precisely controlled by using controlled “living” radical polymerization techniques,^[13] offering a handle to control the local catalytic activity and hence the gel growth. Moreover, it has been demonstrated that polymer brushes show antifouling behavior by preventing the adsorbance of foreign objects, such as nanoparticles and macromolecules, through steric repulsions by polymer chains,^[14] which may provide a solution to the problem of adhesion of gel fibers.

Dr. Y. Wang, Dr. S. Oldenhof, Dr. F. Versluis, M. Shah, Dr. K. Zhang, Dr. V. van Steijn, Dr. R. Eelkema, Prof. J. H. van Esch
Department of Chemical Engineering
Delft University of Technology
van der Maasweg 9, 2629 HZ Delft, The Netherlands
E-mail: r.eelkema@tudelft.nl; j.h.vanesch@tudelft.nl
Prof. X. Guo
State-Key Laboratory of Chemical Engineering
East China University of Science and Technology
Meilong Road 130, 200237 Shanghai, P. R. China
E-mail: guoxuhong@ecust.edu.cn

 The ORCID identification number(s) for the author(s) of this article can be found under <https://doi.org/10.1002/smll.201804154>.

DOI: 10.1002/smll.201804154

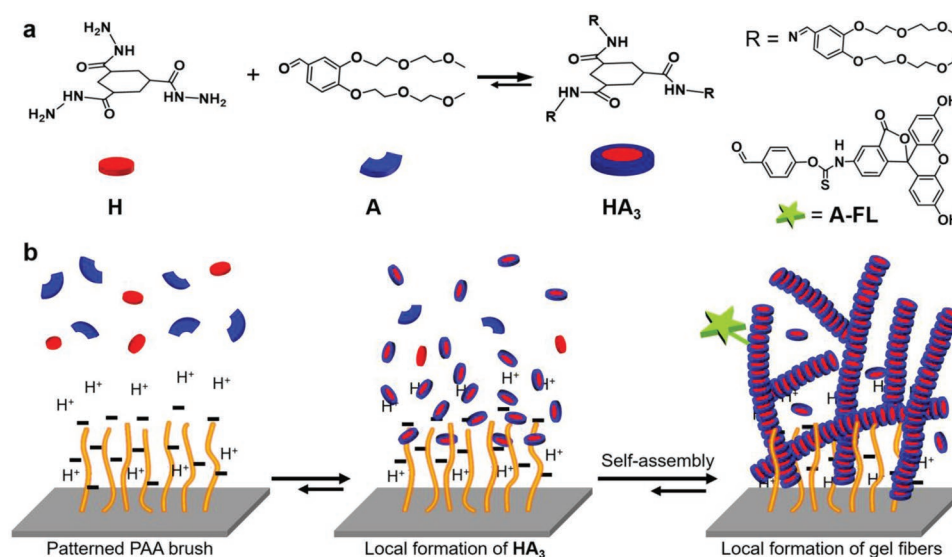


Figure 1. Illustration of localized hydrazone gel formation at the surface of micropatterned PAA brush through the local catalysis formation and self-assembly of HA₃.

Here we investigate if patterned poly(acrylic acid) (PAA) brushes can be used to spatially control the formation of gels through local catalytic formation and self-assembly of HA₃ (Figure 1). We find that gel formation can be precisely controlled in the surface plane with spatial dimensions varying from micro- to centimeter. Importantly, the gels show a preferential growth along the surface normal direction, which can be controlled by tuning the local catalytic activity via simply changing the grafting density of the PAA brushes.

Patterned PAA brushes were prepared by surface-initiated atom-transfer radical polymerization (SI-ATRP) (Supporting information).^[15] To this end, microcontact printing (μ CP) was employed to prepare micropatterns of (3-aminopropyl) triethoxysilane (APTES) on a glass surface.^[16] These APTES patterns were then converted to ATRP initiators by coupling of the amino moieties with α -bromoisobutyryl bromide. These initiator patterns were subsequently used to grow PAA brushes from the monomers of sodium acrylate (Figure S1, Supporting Information). Characterization of the functionalized glass slides by atomic force microscopy showed that the patterns of the stamps, including the shape and dimensions, were precisely transferred to the resultant PAA brushes (Figure S2, Supporting Information). Furthermore, using different concentrations of APTES ink, increasing from 0.5 to 3.0 wt%, during μ CP resulted in brushes with different thicknesses, increasing from 10 to 55 nm, correspondingly (Figure S2, Supporting Information). This clearly shows that the grafting density can be easily controlled by varying the concentration of APTES ink during μ CP.

Since pH is a key parameter for catalyzing the formation of HA₃, we first estimated the electrostatic potential and pH distribution near the brush surface using a simple calculation based on Grahame and Poisson–Boltzmann equations (Supporting Information). The calculations show that a drop in pH from 5.5 in bulk solution to ≈ 3.7 at the brush surface can be obtained (Figure S3, Supporting Information), suggesting a large enough pH difference to catalyze gelator formation preferentially near

the brush surface. In addition, we found that the addition of salt dramatically reduced the pH difference between bulk solution and brush surface due to screening of interfacial charges (Figure S3, Supporting Information). Thus, milli-Q water was used for the gel formation in this study with the aim to obtain a high efficiency of interfacial catalysis.

To examine the local catalysis formation and self-assembly of HA₃ near the brush surface, a glass surface with grafted PAA brushes was brought into contact with a freshly prepared gelator precursor solution composed of 10×10^{-3} M H and 60×10^{-3} M A (a sixfold excess of A was used to ensure full conversion of H to HA₃) in milli-Q water under the protection of a homemade poly(dimethylsiloxane) (PDMS) chamber (Figure S4, Supporting Information). To visualize the growth of gel fibers using confocal laser scanning microscopy (CLSM), 30×10^{-6} M aldehyde modified fluorescein (A-FL) was added to covalently label the gel fibers.^[10a] After an overnight incubation, we found that gel patterns with designed shapes, including squares, lines, rings, and letters, were indeed formed at the brush areas and reproduce with excellent fit of the shapes and dimensions of the parent PAA brushes (Figure 2a,b). Importantly, the pattern dimensions in the interfacial plane can be varied over a broad length scale ranging from micro- to centimeters (Figure 2; and Figure S5, Supporting Information). These experiments indicate that HA₃ are formed and have rapidly self-assembled into gel fibers before diffusing away into the bulk solution. This fast time scale for reaction compared to diffusion results from the efficient local catalysis by the PAA brushes. Nucleation by templates has also been exploited for local growth of supramolecular structures,^[7] however, in our case a separated catalyst-free self-assembly experiment of HA₃ confirms that the PAA brushes did not show nucleation effect on the self-assembly of HA₃ (Figure S6, Supporting Information).

To further investigate the catalytic effect of the brush patterns on local gel formation, we investigated how the growth rate and thickness of the gel patterns can be controlled by the brushes. For this purpose, brush patterns with increasing

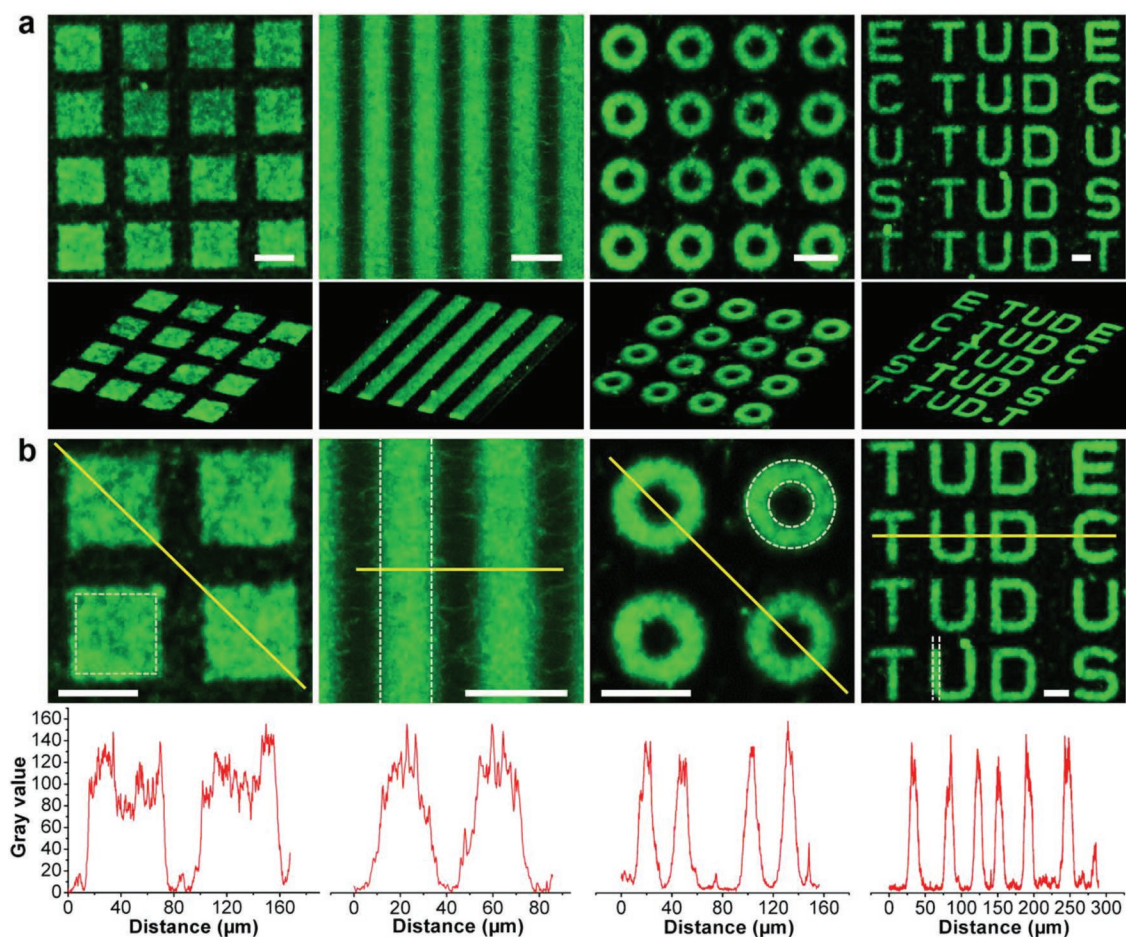


Figure 2. a) Confocal images of gel patterns in different shapes (top: 2D images, bottom: the corresponding 3D images), from left to right are squares, lines, rings, and letters. b) Magnified confocal images of the gel patterns and gray intensity profiles corresponding to the yellow lines on the confocal images; the white dashed lines on the confocal images indicate the corresponding brush areas. Scale bars = 40 μm .

grafting densities, denoted as $B1 < B2 < B3 < B4$, were prepared by performing μCP with 0.5, 1.0, 2.0, and 3.0 wt% APTES inks, respectively. We monitored the growth of gel patterns from these brushes over time by CLSM (Figure 3a). Snapshots of the time series of gels grown from these brushes and time traces of the gel thickness are shown in Figure 3a,b, respectively. It can be seen clearly that increasing the grafting density of PAA brush led to a decrease in the critical growth time of the gel fibers (defined as the time at which the thickness of the gel fibers start to increase) from ≈ 9.0 min for B1 to ≈ 1.5 min for B4 (Figure 3b,c), which can be attributed to the decrease in local pH upon the increase in grafting density of PAA chains. After that, an oriented growth of gel fibers along the surface normal direction was observed (Figure 3a), leading to the formation of 3D gel patterns. However, the gels did not grow infinitely. For instance, in B4, the growth of gel fibers at the brush surface slowed down after ≈ 13 min and effectively halted after ≈ 20 min (Figure 3b,c). Similar growth profiles, though with different time scales, were observed in the samples of B1 to B3 (Figure 3c). The final thickness of the gels was also found to depend on the grafting density and the thickness of PAA brushes, increasing from ≈ 16 μm for B1 (≈ 16.5 nm in thickness) to ≈ 29 μm for B4 (≈ 30 nm in thickness) (Figure 3a,d;

and Figure S7, Supporting Information). The increase of the gel thickness with the grafting density can be attributed to increased acidity of the polymer brushes at higher grafting densities, leading to formation of more HA_3 , thereby resulting in thicker gel layers.

To account for the halted growth and finite gel thickness, we initially hypothesized that this is due to the depletion of the precursor molecules near the catalytic brushes after a certain time of reaction. To test this hypothesis, we performed a gelation experiment in a flow cell to provide a continuous supply of precursor solutions to the brush surface (Figure S8, Supporting Information). However, instead of a continuous gel growth, a growth profile similar to the previous batch experiment was found, indicating that the growth of the gel patterns is not limited by depletion of the precursor molecules. Interestingly, during these flow experiments we noticed that the gel patterns were strongly attached to the PAA brushes, even upon washing vigorously with water (Figure S9, Supporting Information), suggesting the presence of strong interactions between the gel fibers and the brush surfaces. These results are in line with a previous finding, which showed that in acidic condition the hydrazone fibers are protonated and hence slightly positively charged.^[12] Therefore, most likely the electrostatic interactions

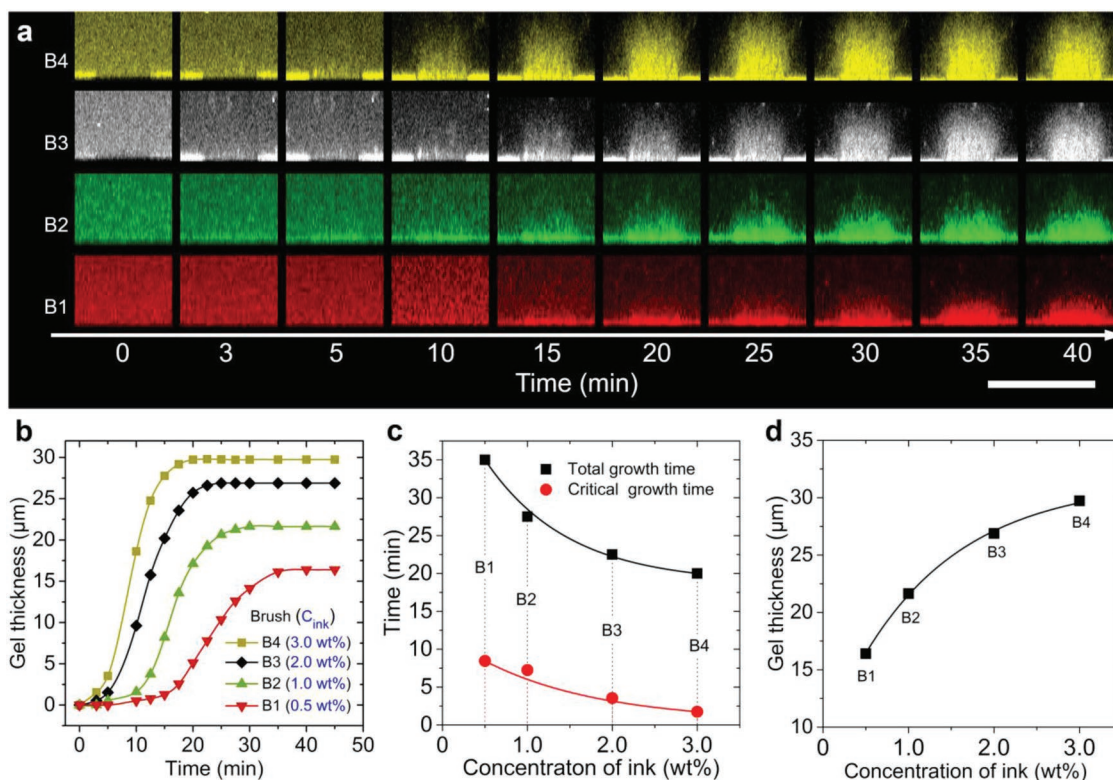


Figure 3. a) Confocal images of the growth of gels in the normal direction of the brush surface, scale bar = 40 μm . b) Variation of gel thickness as a function of grafting density of the PAA brushes. c) The critical growth time (the time that the first fiber was observed) and the total growth time (the time that the gel thickness reached at a plateau) as a function of the brush density. d) The effects of brush density on the final thickness of the gel patterns.

between positively charged fibers and negatively charged PAA brushes are responsible for the adhesion of gel fibers. Given these results, it is reasonable that the physically attached gel fibers make the catalytic brush surface inaccessible for H and A, thus resulting in the limited growth of gel fibers.

The preceding results suggest that our brushes do not present obvious antifouling against the gel fibers due to the presence of electrostatic interactions, which lead us to investigate the mechanism by which gel fibers can be promoted to grow along the normal direction of the brush surface. From the experiments discussed so far, we know that the gelators are always formed preferentially at the brush areas due to the local catalysis. To drive the growth of gels along the normal direction of the brush surface, three kinds of growth mechanisms may play a role (Figure 4a): I) the newly formed gelators diffuse to the top area and add to the upper end of the already formed gel fibers, leading to the growth of new gel fibers from the top area of the old ones. As a result, the fluorescence profile of the gel fibers along the normal direction should extend upward (case I in Figure 4a); II) the new gelators add to the bottom of the already formed gel fibers, thereby pushing the gel fibers upward, in this case, the fluorescence profiles should shift toward the normal direction (case II in Figure 4a); and III) the newly formed gelators diffuse from the catalytic surface into the already formed gel matrix, and nucleate at the old gel fibers, leading to occurrences of branching, bundling, and/or elongation of fibers, which would not only lead to the increase of fluorescence intensity at each location, but also lead to a shift of the

fluorescence profile upward (case III in Figure 4c). To confirm the mechanism of gel growth, we performed a bleaching treatment on the growing gel fibers (Figure 4b). We found that the bleached gel fibers continued to grow from ≈ 15 to ≈ 20 μm in thickness and the fluorescence intensity was increased over time after bleaching, suggesting the addition of new gelators into the previously formed gel fibers. Importantly, upon monitoring the evolution of the fluorescence intensity profile of the gel pattern over time along the surface normal direction, we found the fluorescence intensity was increased from the bottom to the top area (Figure 4d). In addition, the intensity profiles showed a shift along the normal direction, which is in good agreement with case III illustrated in Figure 4a. This can also be confirmed by a two-dye experiment in which later formed aldehyde rhodamine (A-Rh) labeled gel fibers are formed at the sites of previously formed A-FL labeled gel fibers (Figure S10, Supporting Information). These results clearly show that the newly formed gelators diffuse from the brush surface into the previously formed fibers, leading to the increase of fluorescence intensity from the bottom area. The new gelators in turn nucleate at the old fibers and results in branching, bundling, and/or elongation of fibers, thereby leading to the increase in the gel thickness as well as the fiber density. The intensity reached at an equilibrium state within 15 min, however, the fluorescence intensity of the bleached area is still lower than the unbleached pattern (Figure 4c). It thus indicates that the old gel fibers stay at their original position which subsequently block the influx of new H and A and limit the further growth of gel fibers.

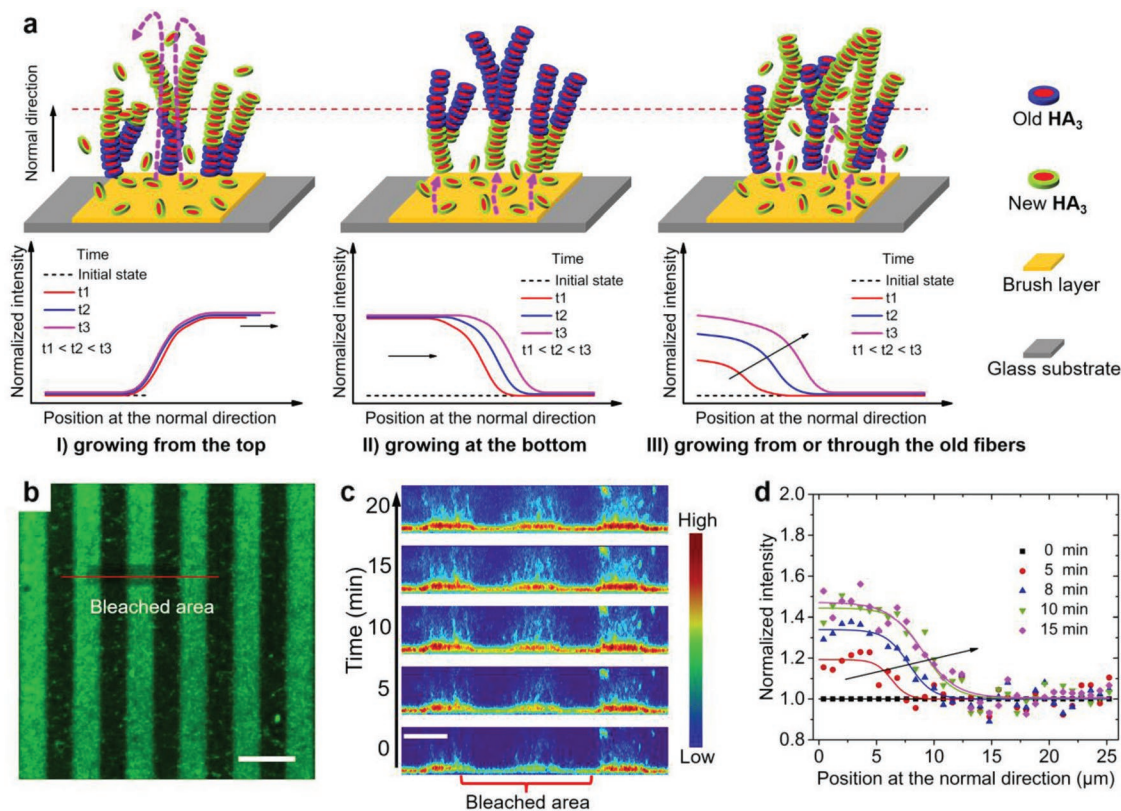


Figure 4. a) Scheme of the possible mechanisms of gel growth from photobleached areas (top) and the corresponding evolution of fluorescence intensity over time along the surface normal direction (bottom). b) Confocal images with bleached area acquired from the surface plane, scale bar = 40 μm . c) Growth of the gel patterns in the surface normal direction after bleaching, scale bar on the left image is 20 μm and the right colour gradient indicates the fluorescence intensity of the gel fibers. d) Spatiotemporal fluorescence intensity curves normalized by the one after bleaching. B2 was used in (b–d).

In conclusion, we have shown the micropatterning of supramolecular gels with controllable spatial dimensions and oriented growth direction through directing the self-assembly of low molecular weight gelators. The efficient local catalysis of micropatterned PAA brushes leading to local formation of gelators enables us to precisely control localized gel formation in different spatial shapes and at broad length scales varying from micro- to centimeter. Importantly, the gel patterns present preferential growth along the normal direction of the brush surface, and their thickness can be easily controlled by simply tuning the grafting density of PAA brushes. We believe this reported “bottom-up” approach for precise control of spatial organization of materials would be of great potential for high-tech applications, for instance, microelectronics, biotherapy, and sensors.

Supporting Information

Supporting Information is available from the Wiley Online Library or from the author.

Acknowledgements

The authors thank Dr. J. M. Poolman for providing H and A; Dr. C. Maity for providing A-FL; Dr. M. Lovrak, and Prof. P. Schaaf from University of Strasbourg for helpful discussion; B. Boshuizen for

XPS measurements; and A. van Langen-Suurling for the fabrication of silicon wafer. They acknowledge China Scholarship Council (CSC) and The Netherland Organization for Scientific Research (NWO VIDI) for funding support.

Conflict of Interest

The authors declare no conflict of interest.

Keywords

directed self-assembly, gels, micropatterning, molecular gelators, supramolecular materials

Received: October 9, 2018
Revised: January 9, 2019
Published online: January 30, 2019

- [1] a) H. Hess, J. L. Ross, *Chem. Soc. Rev.* **2017**, *46*, 5570; b) A. J. Thubagere, W. Li, R. F. Johnson, Z. B. Chen, S. Doroudi, Y. L. Lee, G. Izatt, S. Wittman, N. Srinivas, D. Woods, E. Winfree, L. L. Qian, *Science* **2017**, *357*, eaan6558; c) L. Cera, C. A. Schalley, *Adv. Mater.* **2018**, *30*, 1707029.
[2] R. Galland, P. Leduc, C. Guerin, D. Peyrade, L. Blanchoin, M. Thery, *Nat. Mater.* **2013**, *12*, 416.

- [3] a) W. Z. Li, J. D. Fan, J. W. Li, Y. H. Mai, L. D. Wang, *J. Am. Chem. Soc.* **2015**, *137*, 10399; b) L. L. Han, H. X. Jiang, D. Ouyang, W. C. Chen, T. Hu, J. Y. Wang, S. G. Wen, M. L. Sun, R. Q. Yang, *Nano Energy* **2017**, *36*, 110.
- [4] a) P. K. Kundu, D. Samanta, R. Leizrowice, B. Margulis, H. Zhao, M. Borner, T. Udayabhaskararao, D. Manna, R. Klajn, *Nat. Chem.* **2015**, *7*, 646; b) D. J. Cornwell, O. J. Daubney, D. K. Smith, *J. Am. Chem. Soc.* **2015**, *137*, 15486; c) X. He, J. Fan, J. Zou, K. L. Wooley, *Chem. Commun.* **2016**, *52*, 8455; d) A. S. Groombridge, A. Palma, R. M. Parker, C. Abell, O. A. Scherman, *Chem. Sci.* **2017**, *8*, 1350.
- [5] a) R. J. Williams, A. M. Smith, R. Collins, N. Hodson, A. K. Das, R. V. Ulijn, *Nat. Nanotechnol.* **2009**, *4*, 19; b) R. A. Pires, Y. M. Abul-Haija, D. S. Costa, R. Novoa-Carballal, R. L. Reis, R. V. Ulijn, I. Pashkuleva, *J. Am. Chem. Soc.* **2015**, *137*, 576; c) J. Zhou, X. W. Du, N. Yamagata, B. Xu, *J. Am. Chem. Soc.* **2016**, *138*, 3813; d) J. Zhou, X. Du, B. Xu, *Angew. Chem., Int. Ed.* **2016**, *55*, 5770; e) J. Rodon Fores, M. L. Martinez Mendez, X. Mao, D. Wagner, M. Schmutz, M. Rabineau, P. Lavalle, P. Schaaf, F. Boulmedais, L. Jierry, *Angew. Chem., Int. Ed.* **2017**, *56*, 15984.
- [6] a) I. Ziemecka, G. J. M. Koper, A. G. L. Olive, J. H. van Esch, *Soft Matter* **2013**, *9*, 1556; b) D. Spitzer, V. Marichez, G. Formon, P. Besenius, T. Hermans, *Angew. Chem.* **2018**, *130*, 11519; c) Y. C. Chang, Z. H. Huang, Y. Jiao, J. F. Xu, X. Zhang, *ACS Appl. Mater. Interfaces* **2018**, *10*, 21191.
- [7] a) J. C. Tiller, *Angew. Chem., Int. Ed.* **2003**, *42*, 3072; b) A. M. Bieser, J. C. Tiller, *Chem. Commun.* **2005**, 3942; c) M. G. F. Angelerou, A. Sabri, R. Creasey, P. Angelerou, M. Marlow, M. Zelzer, *Chem. Commun.* **2016**, *52*, 4298.
- [8] a) M. Lovrak, W. E. J. Hendriksen, C. Maity, S. Mytryk, V. van Steijn, R. Eelkema, J. H. van Esch, *Nat. Commun.* **2017**, *8*, 15317; b) M. Lovrak, S. Picken, R. Eelkema, J. van Esch, *ChemNanoMat* **2018**, *4*, 772.
- [9] C. Vigier-Carrière, F. Boulmedais, P. Schaaf, L. Jierry, *Angew. Chem., Int. Ed.* **2018**, *57*, 1448.
- [10] a) J. Boekhoven, J. M. Poolman, C. Maity, F. Li, L. van der Mee, C. B. Minkenberg, E. Mendes, J. H. van Esch, R. Eelkema, *Nat. Chem.* **2013**, *5*, 433; b) J. M. Poolman, J. Boekhoven, A. Besselink, A. G. Olive, J. H. van Esch, R. Eelkema, *Nat. Protoc.* **2014**, *9*, 977.
- [11] A. G. Olive, N. H. Abdullah, I. Ziemecka, E. Mendes, R. Eelkema, J. H. van Esch, *Angew. Chem., Int. Ed.* **2014**, *53*, 4132.
- [12] Y. Wang, F. Versluis, S. Oldenhof, V. Lakshminarayanan, K. Zhang, Y. Wang, J. Wang, R. Eelkema, X. Guo, J. H. van Esch, *Adv. Mater.* **2018**, *30*, 1707408.
- [13] a) J. Pyun, T. Kowalewski, K. Matyjaszewski, *Macromol. Rapid Commun.* **2003**, *24*, 1043; b) S. Edmondson, V. L. Osborne, W. T. Huck, *Chem. Soc. Rev.* **2004**, *33*, 14.
- [14] a) T. McPherson, A. Kidane, I. Szleifer, K. Park, *Langmuir* **1998**, *14*, 176; b) A. Halperin, *Langmuir* **1999**, *15*, 2525; c) I. Szleifer, M. A. Carignano, *Macromol. Rapid Commun.* **2000**, *21*, 423; d) T. Drobek, N. D. Spencer, M. Heuberger, *Macromolecules* **2005**, *38*, 5254.
- [15] a) T. Chen, D. P. Chang, S. Zauscher, *Small* **2010**, *6*, 1504; b) W. Q. Wang, G. H. Ren, W. J. Cai, *RSC Adv.* **2015**, *5*, 60857.
- [16] H. Li, J. Zhang, X. Zhou, G. Lu, Z. Yin, G. Li, T. Wu, F. Boey, S. S. Venkatraman, H. Zhang, *Langmuir* **2010**, *26*, 5603.